



# Enhancement of ethylene production by alkali metal doping of MoVSb mixed oxide catalyst for ethane oxidative dehydrogenation

F. Ivars-Barceló<sup>a,\*</sup>, B. Solsona<sup>b</sup>, E. Asedegbega-Nieto<sup>a</sup>, J.M. López Nieto<sup>c,\*</sup>

<sup>a</sup> Dept. Química Inorgánica y Química Técnica, Facultad de Ciencias, UNED, Av. Espartaco/n, Las Rozas, 28232 Madrid, Spain

<sup>b</sup> Dept. de Ingeniería Química, Universitat de València, C/Dr. Moliner 50, Burjassot, 46100 Valencia, Spain

<sup>c</sup> Instituto de Tecnología Química, Universitat Politècnica de València-Consejo Superior de Investigaciones Científicas, Avenida de los Naranjos s/n, 46022 Valencia, Spain

## ARTICLE INFO

### Keywords:

Ethane  
Ethylene  
Oxidative dehydrogenation  
Mo-V-Sb mixed oxide  
Alkali metals  
Heterogeneous catalysis

## ABSTRACT

Hydrothermally prepared Mo-V-Sb mixed oxides doped with alkali metal cations (Li<sup>+</sup>, Na<sup>+</sup>, K<sup>+</sup>, Rb<sup>+</sup>, or Cs<sup>+</sup>) show a significantly improved catalytic behavior in the oxidative dehydrogenation of ethane (ODH) compared to conventional alkali metal-free MoVSbO catalysts. Initial selectivity to ethylene above 95 % was held up to 20 % of ethane conversion for all alkali metal promoted MoVSbO catalysts, as well as lower ethylene overoxidation at higher ethane conversion, with differences depending on the alkali metal employed. Thus, from Li to K, the enhanced catalytic performance follows a bottom-up trend as increasing the size of the cation. An intermediate behavior is observed though for the catalyst doped with Cs cations, with the highest atomic radius. The K-doped MoVSbO catalyst is the least prone to both ethane total oxidation and ethylene overoxidation, which enables up to 90 % selectivity to ethylene at ethane conversion higher than 65 %.

## 1. Introduction

Ethylene is one of the largest building blocks in the petrochemical industry, reaching over 164 million tons yearly production worldwide in 2018 [1]. However, ethylene is produced by steam cracking of ethane or naphtha, one of the most energy consuming process in chemical industry [2]. In fact, it is an endothermic process which requires operating at high temperature, around 800 °C [3]. In addition, high energy is also required for the separation of reaction products, so that the global process implies a very high demand for energy (ca. 16 GJ/ton<sub>ethylene</sub>) [4]. On the other hand, and from an environmental point of view, very high CO<sub>2</sub> emissions are associated with the olefins production processes (c.a. 1200 gCO<sub>2</sub>/kg<sub>ethylene</sub>) [5], which meant a production of more than 200 million tons of CO<sub>2</sub> in 2018.

Therefore, it seems justified and necessary to develop new alternative methods to produce ethylene [6,7]. In this way, the oxidative dehydrogenation (ODH) of ethane is an interesting alternative as a cheaper and more eco-friendly process [7–11].

In the last decades, several catalytic systems have been proposed to ODH of ethane, where both reaction conditions and mechanisms strongly depend on the catalyst characteristics [7–11]. However, the main drawback in most of catalytic systems is the relatively low

selectivity to ethylene at high ethane conversion or, in other words, the high CO<sub>x</sub> formation by ethylene overoxidation.

Mo-V-Te-(Nb)-O mixed oxides presenting Te<sub>2</sub>M<sub>20</sub>O<sub>57</sub> (M= Mo, V, Nb), the so-called M1 phase, are currently the most promising systems [12–14], since they can operate at relatively low reaction temperatures (300–400 °C) reaching around 75 % yield of ethylene, which is higher than results obtained by steam cracking processes (50–60 %) [7]. Recently, several studies have been reported in order to explain the catalytic performance of M1-containing mixed metal oxides [7,12–20]. Nevertheless, the productivity to ethylene obtained with these catalysts is an aspect to be improved. It must be indicated that these materials were firstly reported as the most effective catalysts in propane selective (amm)oxidation to acrylonitrile or acrylic acid [21–25].

Mo-V-Sb-(Nb)-O catalysts presenting M1 phase similar to that with tellurium-containing ones, are also active and selective for ethane ODH to ethylene [26–30] and for propane selective oxidation to acrylic acid [31–35], although at the moment they are less effective in both reactions than MoVTeNbO catalysts.

The presence of niobium in these kinds of catalysts have been related with a decrease in the number of surface Brønsted acid sites, which has been shown to be a key factor to obtain high selectivity to acrylic acid (in propane oxidation) [32,36], but likely it is also for ethylene selectivity

\* Corresponding authors.

E-mail addresses: [franciscoivars@ccia.uned.es](mailto:franciscoivars@ccia.uned.es) (F. Ivars-Barceló), [jmlopez@itq.upv.es](mailto:jmlopez@itq.upv.es) (J.M. López Nieto).

(in ODH of ethane) since a parallelism seems to exist between both reactions carried out over these kind of catalysts [37]. In fact, the lower surface acidity inherent to the Te-containing catalysts, compared with the corresponding Sb-containing materials [32,36,38], could explain the higher effectiveness of the former ones in both oxidation reactions. In this way, several works have been reported regarding the removal of surface acidity on MoVSbO catalysts by alkali metal incorporation as a good way to improve the catalytic behavior of these materials in propane selective oxidation to acrylic acid [36,38–40]. Thus, it would be interesting to test if a similar effect is found for oxidative dehydrogenation of ethane. Accordingly, this work presents a systematic study on the catalytic behavior of MoVSb mixed oxides catalysts impregnated with alkali metal cations (Li, Na, K and Cs). The influence of both the amount of alkali metal and the activation temperature of the doped sample will be also discussed for the specific case of K, which has shown the best catalytic performance.

## 2. Experimental

### 2.1. Catalyst preparation

The Mo-V-Sb-O mixed oxide was prepared by hydrothermal method from an aqueous gel containing ammonium heptamolybdate, vanadyl sulfate and antimony sulfate in a Mo/V/Sb atomic ratio of 1/0.18/0.15, following a previously reported procedure [40]. The solid obtained was heat-treated at 600 °C for 2 h in N<sub>2</sub> stream, and then it was pore volume impregnated at room temperature with an aqueous solution of the corresponding alkali metal carbonate employing a A/Mo atomic ratio of 0.0025 or 0.0050 [40]. The impregnated materials were finally activated at 500 °C or 600 °C for 1 h in N<sub>2</sub> stream. The resulting catalysts will be named as T-Ax, where T is temperature of activation, A is the alkali metal added (i.e., Li, Na, K, or Cs) and x is 25 or 50 as the catalyst had been doped with A/Mo atomic ratio of 0.0025 or 0.0050, respectively. A non-doped MoVSbO catalyst was also prepared as reference and named MVS.

### 2.2. Catalysts characterization

Chemical analyses of the catalysts were carried out by Inductively Coupled Plasma Atomic Emission Spectroscopy (ICP-AES) with a Varian 715-ES instrument.

The specific surface areas were determined by the Brunauer–Emmett–Teller (BET) method from N<sub>2</sub> adsorption isotherms at 77 K measured on a Micromeritics TriStar 3000 instrument. A desorption treatment at 400 °C (10 °C min<sup>-1</sup> heating rate) for 1 h, at high vacuum range conditions (10<sup>-5</sup>–10<sup>-8</sup> mbar), was conducted for every sample just prior to the isothermal N<sub>2</sub> adsorption analysis.

X-ray diffraction patterns (XRD) were collected using a Philips X'Pert diffractometer equipped with a graphite monochromator, operating at 40 kV and 45 mA, and employing nickel-filtered Cu K $\alpha$  radiation ( $\lambda$  = 0.1542 nm).

The experiments for temperature programmed desorption of ammonia (TPD) were carried out on a TPD/2900 apparatus from Micromeritics. Approximately 0.30 g of sample were pre-treated in a He stream at 450 °C for 1 h. Ammonia was chemisorbed by pulses at 100 °C until equilibrium was reached. Afterwards, a He stream was fluxed for 15 min, prior to increase the temperature up to 500 °C in a He stream of 100 ml min<sup>-1</sup> (heating rate of 10 °C min<sup>-1</sup>). The NH<sub>3</sub> desorption was monitored with both a thermal conductivity detector (TCD), and a mass-spectrometer following the characteristic 15 a.m.u. of ammonia.

### 2.3. Catalytic tests

The catalytic experiments were carried out at atmospheric pressure, in the 340–420 °C temperature range, using a fixed bed quartz tubular reactor (i.d. 20 mm, length, 400 mm). Catalyst samples were introduced

in the reactor diluted with silicon carbide, in order to keep a constant volume in the catalytic bed. The feed consisted of a mixture of C<sub>2</sub>H<sub>6</sub>/O<sub>2</sub>/He with a molar ratio 30/20/50. The amount of catalyst was varied from 0.2 to 2 g in order to obtain several contact times. Reactant and products were analysed by gas chromatography using two packed columns: i) Molecular sieve 5 Å (2.5 m) and ii) Porapak Q (3 m). Blank tests showed no ethane conversion in the temperature range studied.

## 3. Results

### 3.1. Characterization

The bulk chemical analysis of the hydrothermally crystallized MoVSb mixed oxide, before the surface modification with alkali metal cations, provided a Mo/V/Sb molar ratio of 1/0.27/0.15. This means a V/Mo ratio significantly higher than the one employed in the nominal composition of the synthesis gel (1/0.18/0.15), suggesting a preferential incorporation of vanadium into the solid phase precipitating during the hydrothermal synthesis. Since the alkali metal cations were incorporated by incipient wetness impregnation to the respective fraction of the same MoVSbO solid batch (MVS sample), alkali metal/Mo ratios in the final catalysts coincide with the nominal ones. The remaining physico-chemical properties of the catalysts assessed in this work are summarized in Table 1. Some of these features were already reported in previous works based on equivalent catalytic materials for propane selective oxidation [40]. In this sense, representative catalytic properties obtained for propane partial oxidation using some catalysts equivalent to the respective ones here reported are also included (supporting information). The correlation found between them and those for ODH of ethane will be discussed further in detail.

The hydrothermally precipitated MoVSb-containing solid activated at 600 °C in N<sub>2</sub> stream (MVS catalyst) results in a mixture of (Sb<sub>2</sub>O)<sub>2</sub>M<sub>20</sub>O<sub>56</sub> and (Sb<sub>2</sub>O)<sub>2</sub>M<sub>6</sub>O<sub>19</sub> structures (M = Mo+V), the so-called M1 and M2 phases, respectively (Table 1 and Fig. S1), as typically obtained in similar syntheses [26–28,31,34,39–42]. It is known that after modifying the surface of non-doped MoVSbO catalyst by adsorption of lithium, potassium, or cesium cations (A/Mo molar ratio of 2.5·10<sup>-3</sup>) and subsequent activation at 500 °C/N<sub>2</sub>, no significant changes in the crystalline-phase distribution were observed in the resulting catalysts (Fig. S1) [40]. However, in our case, the activation at 600 °C/N<sub>2</sub> of equivalent alkali metal doped materials (A/Mo = 0.0025) led to a partial decomposition of M1 and M2 phases into Sb<sub>2</sub>Mo<sub>10</sub>O<sub>31</sub> structure, except for the Cs-doped catalyst (Table 1 and supporting information, Fig. S1). In this sense, M1 and M2 partial decompositions took place in different proportion depending on the nature of the alkali metal. Quantitative phase analysis applying Rietveld method on the X-ray diffractograms, for each alkali metal doped material activated at 600 °C, shows a consistent tendency for M1 and M2 phases decomposition by decreasing the ionic radius of the alkali metal, as it is displayed in Fig. 1.

The M1 phase experiences a higher decomposition with a linear response for the whole alkali metal ionic radius range, while the M2 phase decomposes also linearly but until sodium, from which the decomposition degree stabilizes. The linear response includes no depletion of M1 and M2 phases detected for the equivalent Cs-doped catalyst (600-Cs25). The percentage of phase decomposition has been calculated with respect to the non-doped Mo-V-Sb mixed oxide (MVS).

Doping the MoVSb mixed oxide by a twofold increase in the alkali-metal/Mo molar ratio (A/Mo = 5·10<sup>-3</sup>) was conducted using K<sup>+</sup>, as representative alkali-metal cation due to its intermediate ionic radius within the IA-group (Table 1). Consecutive activation at 600 °C/N<sub>2</sub> led also to partial decomposition of original M1 and M2 phases in the resulting catalyst (600-K50). However, instead of Sb<sub>2</sub>Mo<sub>10</sub>O<sub>31</sub>, the new phase forming in this case was orthorhombic molybdate (MoO<sub>3</sub>-ortho) (Table 1 and supporting information, Fig. S1).

Surface acid properties of the Mo-V-Sb mixed oxide catalyst, and derivative catalysts obtained by impregnation with alkali metal cations

**Table 1**  
Main characteristics of the non-doped and alkali metal doped Mo-V-Sb oxide catalysts prepared.

Catalysts	$S_{\text{BET}}^a$	$\text{NH}_3\text{-TPD}^b$			Ethane ODH <sup>c</sup>			STY <sup>d</sup> ( $\text{g}_{\text{C}_2\text{H}_4} \text{h}^{-1} \text{kg}_{\text{cat}}^{-1}$ )	Crystalline phases <sup>e</sup> (DRX)	
		( $\mu\text{mol g}^{-1}$ )	$T_{\text{max}}$	$\Delta H_{\text{ads}}$	Conv.	$S_{\text{C}_2\text{H}_4}$	$S_{\text{CO}}$			$S_{\text{CO}_2}$
MVS	14.0	320.6	214	139.0	33.2	87.8	8.6	3.6	204	M1, M2
600-Li25	4.9	9.8	175	128.1	22.6	93.6	3.6	2.7	148	M1, M2, $\text{Sb}_2\text{Mo}_{10}\text{O}_{31}$
600-Na25	6.8	68.0	175	128.3	32.9	93.8	4.0	2.3	216	M1, M2, $\text{Sb}_2\text{Mo}_{10}\text{O}_{31}$
600-K25	10.5	108.1	191	132.2	40.9	93.6	4.5	1.9	268	M1, M2, $\text{Sb}_2\text{Mo}_{10}\text{O}_{31}$
600-Cs25	7.5	77.2	180	129.4	35.2	92.8	4.0	3.2	229	M1, M2
500-K25	10.8	91.8	190	132.9	26.8	93.7	2.9	3.4	176	M1, M2
600-K50	-	-	-	-	38.8	89.0	7.6	2.4	242	M1, M2, $\text{MoO}_3\text{-ortho}$

<sup>a</sup> Surface area determined by BET isotherm of  $\text{N}_2$  adsorption. Non-doped  $\text{MoVSbO}$  catalyst is also included as reference.

<sup>b</sup>  $\text{NH}_3$  amount per gram of catalyst (in  $\mu\text{mol g}^{-1}$ ) adsorbed in steady state at  $100^\circ\text{C}$  during TPD experiment (measured in standard conditions of pressure and temperature). Temperature of maximum desorption rate ( $T_{\text{max}}$ ,  $^\circ\text{C}$ ) during  $\text{NH}_3\text{-TPD}$  experiments, and  $\text{NH}_3$  adsorption enthalpy calculated ( $\Delta H_{\text{ads}}$ ,  $\text{kJ mol}^{-1}$ ).

<sup>c</sup> Results obtained during oxidative dehydrogenation of ethane at  $400^\circ\text{C}$  and a contact time, W/F, of  $40 \text{ g}_{\text{cat}} \text{h} (\text{mol}_{\text{C}_2\text{H}_6})^{-1}$ . Conversion of ethane (Conv., %), and selectivity to carbon-based products ( $S_x$ , %).

<sup>d</sup> Formation of ethene per unit mass of catalyst and per unit time, STY, at  $400^\circ\text{C}$ , in  $\text{g}_{\text{C}_2\text{H}_4} \text{h}^{-1} \text{kg}_{\text{cat}}^{-1}$ .

<sup>e</sup> Major crystalline phases detected by powder XRD: M1 =  $(\text{Sb}_2\text{O})\text{M}_{20}\text{O}_{56}$ ; M2 =  $(\text{Sb}_2\text{O})\text{M}_6\text{O}_{19}$  ( $M = \text{Mo}, \text{V}$ );  $\text{Sb}_2\text{Mo}_{10}\text{O}_{31}$  [JCPDS: 33–105]; orthorhombic o-  $\text{MoO}_3$  [JCPDS: 5–508].

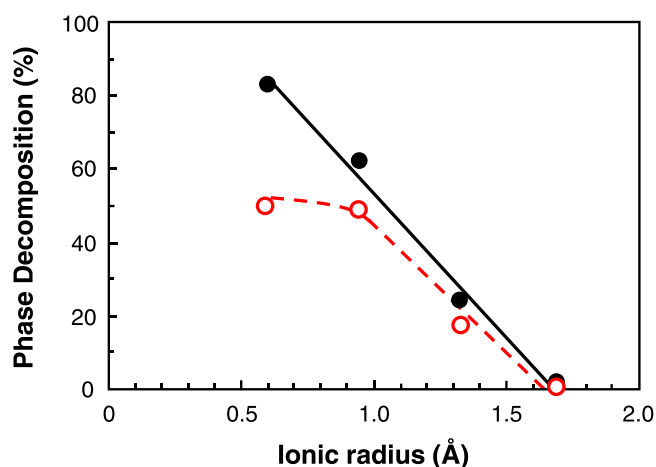


**Fig. 1.** Variation of the decomposition of M1 (●) and M2 (○) phases during the activation at  $600^\circ\text{C}/\text{N}_2$  of the alkali metal doped  $\text{MoVSb}$  mixed oxide catalysts, with the ionic radius of the alkali metal cation employed:  $\text{Li}^+$  (0.60 Å),  $\text{Na}^+$  (0.95 Å),  $\text{K}^+$  (1.33 Å),  $\text{Cs}^+$  (1.69 Å).

and activated at  $600^\circ\text{C}/\text{N}_2$  or  $500^\circ\text{C}/\text{N}_2$ , were investigated by temperature programmed desorption of  $\text{NH}_3$  (TPD- $\text{NH}_3$ ) chemisorbed under equilibrium conditions at  $100^\circ\text{C}$ . From TPD- $\text{NH}_3$  results (Fig. 2, Table 1, and supporting information, Fig. S2), it can be observed that for all alkali metal doped catalysts the intensity of the TPD- $\text{NH}_3$  curve decreases drastically with respect to the non-doped Mo-V-Sb mixed oxide (MVS catalyst). This fact implies a strong reduction in the number of surface acid sites for the modified catalysts regardless of the alkali-metal cation incorporated or activation temperature employed. However, some differences were observed between both series of catalysts since the alkali metal doped catalysts activated at  $600^\circ\text{C}$  showed a tendency in the number of acid sites per mass of sample depending on the alkali metal used (Fig. 2 and Table 1), whereas no significant variation appears in the ones activated at  $500^\circ\text{C}$  (supporting information, Fig. S2).

Within the  $600^\circ\text{C}$  activation series, the highest drop in surface acid sites is observed for the catalyst modified with  $\text{Li}^+$  (600-Li25), with 97 % less acid sites per gram compared with the MVS sample (Table 1). While it is true that the 600-Li25 catalyst also undergoes the strongest reduction of surface area, this is just about 3 times lower than the MVS sample, which cannot explain by itself the more than 32 times lower density of surface acid sites of the former one compared with the latter one. The 600-Li25 catalyst also presents the highest decomposition degree for M1 and M2 phases, which seems directly related to the drop

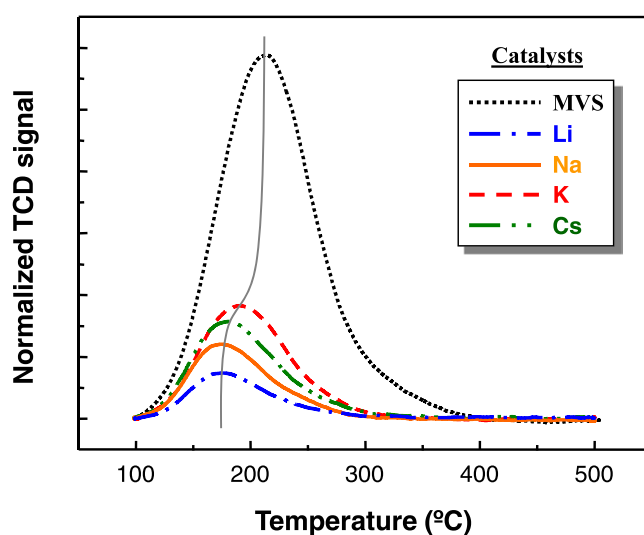


**Fig. 2.** TPD- $\text{NH}_3$  curves (normalized per mass unit) of alkali metal doped  $\text{MoVSb}$  mixed oxide catalysts ( $A/\text{Mo} = 0.0025$ ;  $A = \text{Li}, \text{Na}, \text{K}$  or  $\text{Cs}$ ) activated at  $600^\circ\text{C}$ . Comparatively, the non-doped  $\text{MoVSb}$  mixed oxide catalyst (sample MVS) is also included. Detailed experiment conditions are in experimental section.

of both its surface area and acid sites. Nevertheless, the opposite site, with no phase decomposition detected for the 600-Cs25 catalyst, also presents important reduction in either surface area or the number of surface acid sites, ca. 46 % and 76 %, respectively, compared with the non-doped Mo-V-Sb mixed oxide (MVS catalyst). Therefore, although partial decomposition of M1 and M2 phases must be influencing, it is not the unique factor. This is confirmed as well by the results for the catalysts doped with Na or K cations, with intermediate ionic radius. Thus, the 600-Na25 catalyst, with important M1 and M2 decomposition (Fig. 1), shows ca. 51 % and 79 % reduction in surface area and density of acid sites, respectively, very similar to the 600-Cs25 catalyst with no phase decomposition. Finally, the 600-K25 catalyst, also presenting M1 and M2 phase partial decomposition, appears by far as the alkali metal doped catalyst with the lowest decrease in surface area and density of acid sites, ca. 25 % and 66 %, respectively (Table 1). Therefore, the upward trend in the number of surface acid sites for the alkali metal doped catalysts activated at  $600^\circ\text{C}$ , depending on the alkali metal cation employed, results as follows:  $\text{Li} > \text{Na} > \text{Cs} > \text{K}$ .

The 600-K25 catalyst also shows the highest temperature for the maximum  $\text{NH}_3$  desorption rate among all the alkali doped catalysts

(Table 1 and Fig. 2). In this sense, when no activation energy is needed for the adsorption of  $\text{NH}_3$ , as it is here the case, the activation energy for the  $\text{NH}_3$  desorption process, which match with the adsorption enthalpy, is directly associated to the acid strength [43,44]. Therefore, the maximum desorption temperature is proportional to the acid strength of the surface sites and, in all the alkali metal doped catalysts prepared, appears significantly lower than for the non-doped Mo-V-Sb mixed oxide (MVS catalyst), as it was expected [40,45–50]. In terms of acid strength determined by  $\text{NH}_3$ -TPD, three categories are typically distinguished: weak, medium, and strong sites; related to the energy range for the differential heat of  $\text{NH}_3$  adsorption, *i.e.*, 90–120, 120–150, and  $> 150 \text{ kJ mol}^{-1}$ , respectively. Thus, adsorption enthalpies were calculated from the  $\text{NH}_3$ -TPD results (Table 1), and absolutely all the samples, regardless of the variations among them, can be classified as medium acid sites. The highest adsorption enthalpy, and so surface acid strength, is given by the non-doped Mo-V-Sb mixed oxide (MVS catalyst), with  $139 \text{ kJ mol}^{-1}$ . The acid strength immediately below corresponds to the K-doped catalysts (500-K25 and 600-K25 samples), both with similar  $\text{NH}_3$  adsorption energy around  $132.5 \text{ kJ mol}^{-1}$  regardless of the temperature employed during the activation treatment. The surface acid strength for the rest of alkali metal doped catalysts appears lower, although the small differences between them do not allow to establish any significant trend. Nevertheless, it can be said that, compared with the shortest lessening in adsorption enthalpy found for the K-doped catalysts, around  $6.5 \text{ kJ mol}^{-1}$ , the downward difference for the rest of alkali metal doped catalysts is significantly longer, with net values of  $10.25 \pm 0.65 \text{ kJ mol}^{-1}$  (Table 1).

### 3.2. Catalytic behavior in ethane ODH

The effect of the nature and amount of alkali metal on the MoVSb mixed metal oxide, and the temperature (500 or 600 °C) for the heat-treatment after the alkali metal impregnation, on the catalytic behavior of these materials for the oxidative dehydrogenation of ethane, has been studied. The main results are summarized in Table 1. In the case of K-doped catalysts, Fig. 3 shows the ethane conversion (at a contact time of  $40 \text{ g}_{\text{cat}} \text{ h mol}_{\text{C}_2\text{H}_6}^{-1}$ ) and the selectivity to ethylene (at ethane iso-conversion of 40 %) obtained during ODH of ethane at 400 °C with potassium doped catalysts (K/Mo= 0.0025) heat-treated at 500 or

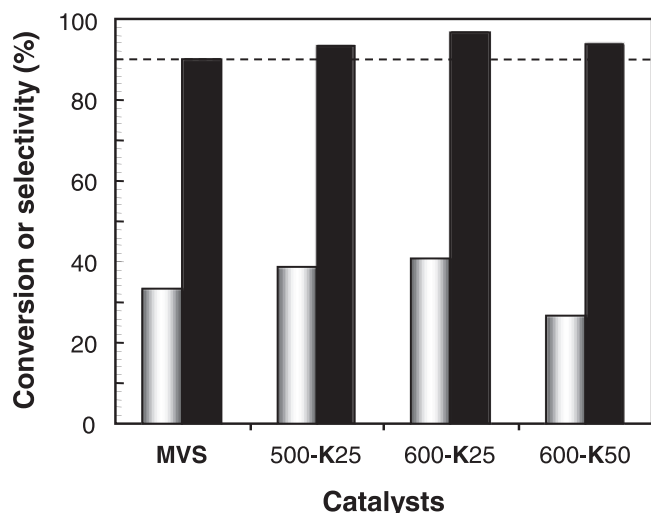


Fig. 3. Ethane conversion at a contact time, W/F, of  $40 \text{ g}_{\text{cat}} \cdot \text{h} / \text{mol}_{\text{C}_2\text{H}_6}$  (white bars) and selectivity to ethylene at ethane iso-conversion of 40 % (black bars) during ODH of ethane with K-doped MoVSbO catalysts. The non-doped MoVSbO catalyst (MVS) is also included as reference. In all cases, data standard deviation was found below 2.1 % for conversion, and below 1.3 % for selectivity. Reaction conditions: Temperature= 400 °C; Molar ratio of  $\text{C}_2\text{H}_6/\text{O}_2/\text{He} = 30/20/50$ .

600 °C/ $\text{N}_2$  (500-K25 and 600-K25 samples), or with double potassium content (K/Mo= 0.005) and heat-treated at 600 °C (600-K50 sample). For comparison, it is also included the non-doped MoVSb mixed oxide catalyst (sample MVS).

The selectivity to ethylene at ethane iso-conversion improves for all K-doped catalysts, compared with the non-doped MoVSb oxide material, regardless of the alkali metal load or activation temperature employed. For the catalysts doped with a K/Mo molar ratio of 0.0025, even the ethane conversion is enhanced. However, the highest content of potassium (K/Mo= 0.0050) seems to have a negative influence on the catalytic activity since ethane conversion for the 600-K50 catalyst is even lower than that for the non-doped MVS catalyst. By contrast, the catalyst doped with K/Mo of 0.0025 and heat-treated at 600 °C/ $\text{N}_2$  shows both the highest ethane conversion and selectivity to ethylene.

To better understand the catalytic behavior of these K-doped catalysts, the variation of the selectivity to ethylene with the ethane conversion is shown in Fig. 4. From these results, it can be clearly confirmed that, with respect to the non-doped catalyst, the selectivity to ethylene is improved for all K-doped catalysts along all the range of the alkane conversions studied.

At initial ethane conversion, the selectivity to ethylene tends to values above 97 % and the differences among catalysts are small. Nevertheless, these differences are progressively more glaring as ethane conversion increases. The most selective catalysts in all the range of ethane conversion studied were those activated at 600 °C. Thus, selectivities to ethylene appear no lower than 90 % on 600-K50 and 600-K25 catalysts up to 50 % and 60 % ethane conversion, respectively.

The most selective K-doped MoVSb mixed oxide catalyst (600-K25), at the highest alkane conversions, was selected to be compared with the other alkali metal (Li, Na and Cs) doped catalysts prepared using the equivalent conditions (alkali metal/Mo= 0.0025 and heat-treated at 600 °C/ $\text{N}_2$ ). The ethane conversion (at a contact time of  $40 \text{ g}_{\text{cat}} \text{ h mol}_{\text{C}_2\text{H}_6}^{-1}$ ) and the selectivity to ethylene at alkane iso-conversion of 40 %, obtained during ODH of ethane at 400 °C with these catalysts, are shown in Fig. 5.

The selectivity to ethylene at ethane iso-conversion for all the alkali metal doped catalysts is higher than that for the non-doped one. This enhancement appears to follow a trend, so that the higher the atomic number of the doping alkali metal the higher the selectivity to ethylene, until reaching a maximum for the K-doped catalyst to fall back with Cs doping (Fig. 5). A similar trend is observed for the ethane conversion, although in this case, the starting point with the Li-doped catalyst

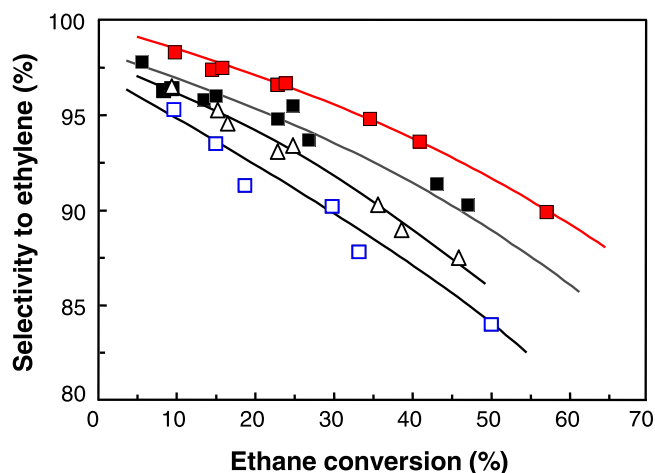
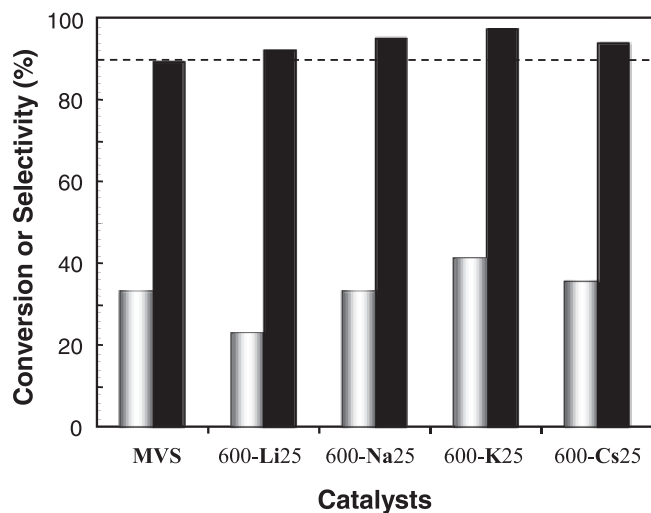


Fig. 4. Variation of the selectivity to ethylene with ethane conversion, during ODH of ethane over the K-doped MoVSb mixed oxide catalysts: 500-K25 ( $\Delta$ ), 600-K25 ( $\blacksquare$ ), and 600-K50 ( $\blacktriangle$ ), and the non-doped MoVSb mixed oxide catalyst (MVS) ( $\square$ ). Reaction conditions: Temperature = 400 °C; molar ratio of  $\text{C}_2\text{H}_6/\text{O}_2/\text{He} = 30/20/50$ .



**Fig. 5.** Ethane conversion at a contact time,  $W/F$ , of  $40 \text{ g}_{\text{cat}} \text{ h mol}_{\text{C}_2\text{H}_6}^{-1}$  (white bars), and selectivity to ethylene at ethane iso-conversion of 30 % (black bars), during ODH of ethane with alkali metal doped MoVSb mixed oxide catalysts (Alkali metal/Mo = 0.0025; activation at  $600 \text{ }^\circ\text{C}/\text{N}_2$ ). The non-doped MoVSb mixed oxide catalyst (MVS) is also included as reference. In all cases, data standard deviation was found below 2.1 % for conversion, and below 1.3 % for selectivity. Reaction conditions: Temperature =  $400 \text{ }^\circ\text{C}$ ; Molar ratio of  $\text{C}_2\text{H}_6/\text{O}_2/\text{He} = 30/20/50$ .

appears below the conversion reached by the non-doped one. This could be related to the low surface area presented by the Li-doped catalyst compared with the rest of materials (Table 1). Indeed, comparing the specific catalytic activity instead (Fig. 6), this is significantly higher (about double) for the Li-doped catalyst, keeping up with all the other alkali metal doped catalysts, than for the non-doped catalyst. While the differences in ethane conversion depending on the alkali metal employed appear within the 20–40 % range, for the specific catalytic activity the differences among the doped catalysts are meaningless (Fig. 6).

Fig. 7 shows the variation of the selectivity to ethylene with the ethane conversion, obtained during ODH of ethane with the different alkali metal doped MoVSbO catalysts activated at  $600 \text{ }^\circ\text{C}$ . Comparatively, results of the non-doped MoVSbO catalyst are also included (sample MVS). It is observed that, whatever the alkali metal

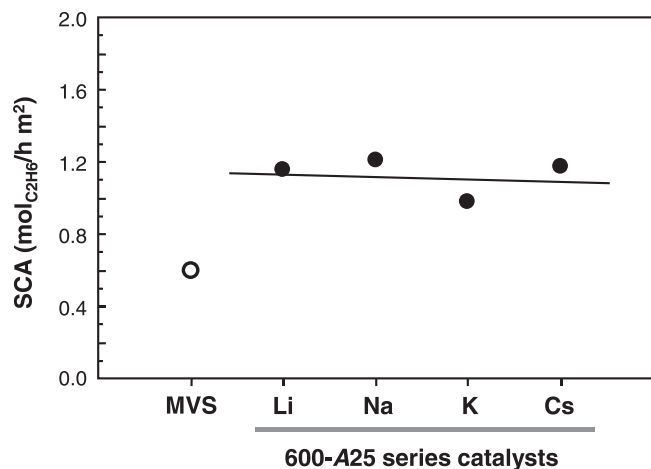


**Fig. 6.** Specific catalytic activity (SCA, in  $\text{mmol}_{\text{C}_2\text{H}_6} \text{ h m}^{-2}$ ) during ODH of ethane at a contact time,  $W/F$ , of  $40 \text{ g}_{\text{cat}} \text{ h mol}_{\text{C}_2\text{H}_6}^{-1}$  over alkali metal doped MoVSbO catalysts (Alkali metal/Mo = 0.0025; activation at  $600 \text{ }^\circ\text{C}/\text{N}_2$ ). The non-doped MoVSbO catalyst (MVS) is also included as reference. Reaction conditions: Temperature =  $400 \text{ }^\circ\text{C}$ ;  $\text{C}_2\text{H}_6/\text{O}_2/\text{He}$  molar ratio of 30/20/50.

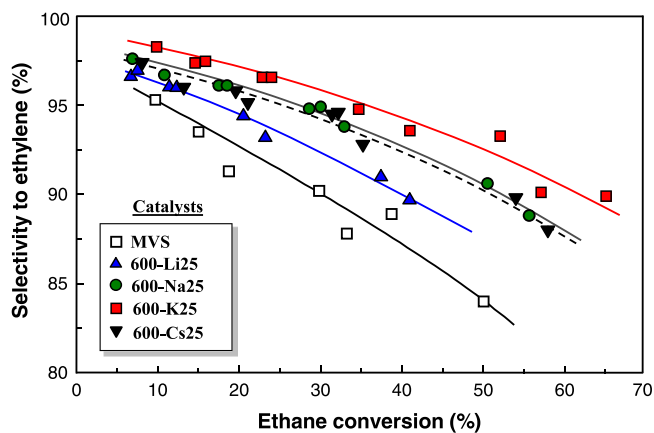


**Fig. 7.** Variation of the selectivity to ethylene with ethane conversion, obtained during ODH of ethane over alkali metal doped MoVSb mixed oxide catalysts (Li, Na, K or Cs) activated at  $600 \text{ }^\circ\text{C}/\text{N}_2$ . The non-doped MoVSb mixed oxide catalyst (MVS) is also included as reference. Reaction conditions: Temperature =  $400 \text{ }^\circ\text{C}$ ;  $\text{C}_2\text{H}_6/\text{O}_2/\text{He}$  molar ratio of 30/20/50.

incorporated by impregnation, an enhanced catalytic behavior in ODH of ethane is obtained, presenting higher selectivity to ethylene than the non-doped MoVSbO catalyst. This takes place for the whole range of ethane conversion studied, with the K-doped MoVSb mixed oxide as the most effective catalyst. In general, the selectivity to ethylene is very high in all alkali metal doped catalyst presented, with little differences among them, especially at low ethane conversion. It is necessary to enlarge y-axis, as displayed in Fig. 7, to clearly appreciate the differences among the distinct catalysts, so that the selectivity to ethylene follows the upward trend:  $\text{MVS} < 600\text{-Li}25 < 600\text{-Na}25 \sim 600\text{-Cs}25 < 600\text{-K}25$ .

It is important to mention that after 48 h of reaction at  $400 \text{ }^\circ\text{C}$ ; the longest period experimentally studied in this work; no deactivation was observed in any of the catalysts tested.

#### 4. Discussion

MoV-based mixed oxides with M1-type structure have been generally reported as active catalysts for partial oxidation of light alkanes ( $\text{C}_2\text{-C}_4$ ) [15,18,27,37,42]. The reaction mechanism for the light alkane activation in this kind of catalyst has shown to be unique regardless of the alkane fed, being the formation of the corresponding olefin the first step, followed by the allylic oxidation intermediate to generate the final partial oxidation product [37]. In the case of ethane, there is no allylic position in the resulting olefin, so the reaction stops at ethylene which appears as the main partial oxidation product. Thus, according to the presented results, ethylene is a primary reaction product to which these catalysts have shown extremely high selectivity at low ethane conversion. The selectivity to ethylene decreases progressively as increasing ethane conversion, due to ethylene overoxidation into  $\text{CO}_x$ .

The smallest alkane giving rise to an olefine containing allylic position, susceptible to be consecutively oxidized, is propane. In this sense, selective oxidation of propane employing alkali metal doped MoVSbO catalysts equivalent to those here studied has been previously reported, yielding acrylic acid as main partial oxidation product [40]. Acrylic acid appears as a secondary product with low initial selectivity which grows up as increasing propane conversion. Until reaching a maximum, the selectivity decreases for higher propane conversion due to acrylic acid overoxidation by consecutive reactions.

Considering that the formation of acrylic acid at low propane conversions minimizes the presence of undesired overoxidation reactions, a first approximation to evaluate the behavior of these catalysts would be the study of the possible parallelism between the formation of ethylene from ethane, and the formation of acrylic acid from propane. In this way, the catalytic results presented here for ethane ODH have been compared

with those previously reported on propane partial oxidation to acrylic acid with equivalent alkali metal doped MoVSbO catalysts (supporting information, Table S1) [40]. Fig. 8 shows the results for the selectivity to the main reaction product for each reaction (ethylene from ethane ODH, and acrylic acid from propane partial oxidation) at alkane iso-conversion conditions, appearing a similar tendency for the catalyst effectivity regardless of the nature of the main partial oxidation product obtained in both reactions.

It must be pointed out that the alkane iso-conversion for the comparison (30 %) was selected within the optimum range for the acrylic acid (a secondary product) formation, which does not match that for the highest ethylene (a primary product) selectivity [37–40,50], due to the different reactivity of the olefin formed in each respective process.

The parallelism found between these two products (ethylene from ethane and acrylic acid from propane), from different oxidation reactions on equivalent alkali metal doped MoVSb mixed oxide catalysts, confirm an identical alkane activation mechanism to form the corresponding olefin on this kind of catalytic system; regardless of the alkane employed [37]; and the different olefin reactivity. Thus, once the olefine is formed, the next step in the reaction mechanism, over these Mo-V-based mixed oxide catalyst, is the selective attack to remove an allyl hydrogen of the corresponding olefin, avoiding vinyl hydrogens. This is possible for propylene, but not for ethylene (without allyl hydrogen). Therefore, the consecutive transformation of propylene proceeds to give rise the corresponding allylic oxidation intermediate, precursor of the acrylic acid final product, while ethylene transformation into higher partial oxidation states is irretrievably halted [37].

In both reactions (propane and ethane oxidation) an important enhancement to desired partial oxidation products is observed when very low amount of alkali metal cations is directly added on the surface of a MoVSb mixed oxide catalyst mainly containing the so-called M1 phase (Table 1, and supporting information, Table S1). The improvement in selectivity to acrylic acid (for propane oxidation) by the incorporation of alkali metal cations has been related to the elimination of non-selective strong acid sites on the catalyst surface, responsible for combustion products' formation, CO and CO<sub>2</sub> [36,38,40,47]. In this sense, a similar effect seems to exist in selectivity to ethylene during ODH of ethane at high ethane conversion, according to the results presented in Table 1. This table includes the selectivity to all carbon-based products detected for ethane ODH (ethylene, CO, and CO<sub>2</sub>) on the most

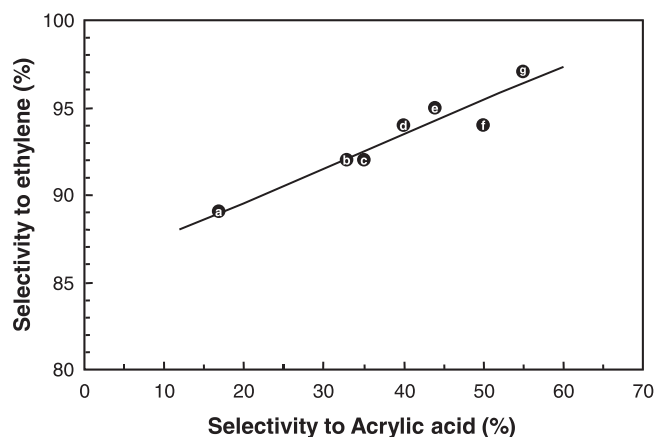


Fig. 8. Selectivity to ethylene (for ODH of ethane) versus selectivity to acrylic acid (for selective propane oxidation) obtained with the alkali metal doped MoVSb mixed oxide catalysts (Alkali metal/Mo= 0.0025) presented in this paper (Table 1). Both, the selectivity to acrylic acid from propane and the selectivity to ethylene from ethane, were obtained for alkane iso-conversion of ca. 30 %. Results for propane oxidation from ref. [40]. Catalyst symbols: MVS (a), 600-Li25 (b), 500-K25 (c), 600-Cs25 (d), 600-Na25 (e), 600-K50 (f), 600-K25 (g).

representative catalysts tested at the corresponding ethane conversions obtained setting a reaction temperature of 400 °C.

As expected, the selectivity to CO<sub>x</sub> for the non-doped MoVSb mixed oxide catalyst (MVS sample) appears significantly higher than for any of the alkali metal doped catalysts tested at equivalent or even higher ethane conversion (Table 1). Among the carbon-based combustion products, the strongest drop in selectivity appears especially on CO, in favor of ethylene, for the alkali metal doped catalysts activated at 600 °C. Nevertheless, it is important to point out the exception for the most effective catalyst, 600-K25, for which the selectivity of both CO and CO<sub>2</sub> undergo identical 47 % degree of reduction with respect to the non-doped MVS catalyst. CO presents higher selectivity than CO<sub>2</sub> for the whole range of ethane conversion obtained on the MVS sample (Fig. 9). A meaningful linear correlation between the selectivity to either CO or CO<sub>2</sub>, and the ethane conversion, over the MVS catalyst, can be stated from the R-squared value (above 0.8) for both fitting equations in Fig. 9. The higher slope for the fitting line equation of CO selectivity (0.15), compared with that for CO<sub>2</sub> (0.09), indicates a higher dependence on ethane conversion for CO. On the other hand, extrapolation to zero ethane conversion for the fitting line equations of CO and CO<sub>2</sub> selectivities give rise to 2.8 and 0.3 values, respectively. A trend to zero selectivity at zero ethane conversion, observed for the CO<sub>2</sub>, is indicative of a secondary product, what in this case implies the CO<sub>2</sub> formation from consecutive oxidation of the ethylene product. Meanwhile, the trend significantly distinct to zero for the CO selectivity at zero ethane conversion is characteristic of a primary product, evoking the CO formation directly from ethane total oxidation. Nevertheless, additional CO formation from ethylene overoxidation cannot be discarded. In fact, the higher proportion of variation in the CO<sub>2</sub> selectivity that can be attributed to the ethane conversion (R<sup>2</sup> = 0.97), compared with that for the CO (R<sup>2</sup> = 0.85), would be in good agreement with just one contributing reaction for CO<sub>2</sub> formation, and more than one contribution for the CO formation.

Therefore, since all alkali metal doped catalysts activated at 600 °C present a stronger reduction in CO selectivity, the doping on these catalysts must be especially influencing the active sites forming this primary combustion product, regardless of the additional effect on the active sites responsible for the ethylene overoxidation into CO<sub>2</sub>. The suppression of ethylene total oxidation is minimum for Cs (600-Cs25 catalyst), followed by Li (600-Li25 catalyst) and Na (600-Na25 catalyst) until reaching the maximum for the K-doped catalyst (600-K25) with a suppression of CO<sub>2</sub> formation proportional to that for the CO formation (Table 1). On the other hand, comparing the most effective 600-K25 catalyst with the equivalent K-doped one activated at lower temperature

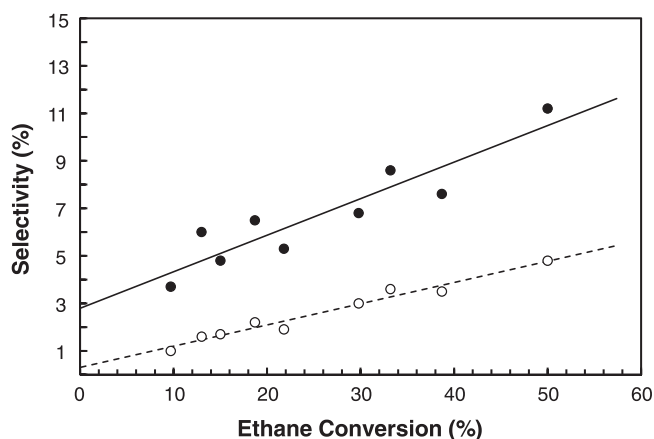


Fig. 9. Variation of the selectivity to CO (●) or CO<sub>2</sub> (○) with ethane conversion, obtained during ODH of ethane over the non-doped MoVSb mixed oxide catalyst (MVS). Fitting line equations:  $y = 0.15x + 2.79$  ( $r^2 = 0.85$ ) for CO;  $y = 0.09x + 0.30$  ( $r^2 = 0.97$ ) for CO<sub>2</sub>. Reaction conditions: Temperature range= 340–400 °C; C<sub>2</sub>H<sub>6</sub>/O<sub>2</sub> molar ratio 1.5.

(500-K25 catalyst), the drop in the selectivity to  $\text{CO}_x$ , at ethane isoconversion of ca. 40 %, is significantly shorter for the latter one. This is mostly due to the meaningless effect of this 500-K25 catalyst on reducing the selectivity to CO (Table 1). Therefore, the activation temperature at 600 °C appears to be key to get the suppression of the total combustion of ethane into CO on these K-doped catalysts.

Unfortunately, there are no meaningful differences in the surface acid properties investigated by  $\text{NH}_3$ -TPD (Table 1), on these K-doped catalysts activated at 500 °C (500-K25) or 600 °C (600-K25), that could explain the significant distinction between them in terms of suppression of CO formation. Therefore, this distinct behavior might be most likely coming from changes on redox sites (number and/or properties) induced by the partial decomposition of crystalline phases occurring for the highest activation temperature (Table 1 and Fig. 1). Nevertheless, it should not be forgotten that this partial decomposition in the doped catalysts activated at 600 °C also induced important changes in their surface acid properties. In fact, a correlation between the density of acid sites on these catalysts and the type of alkali metal cation employed is evidenced in Fig. 2, in contrast with no trend observed for those catalysts activated at 500 °C (supporting information, Fig. S2). In this sense, comparing the selectivity to ethylene (obtained at iso-conversion conditions) with the density of acid sites for the doped catalysts undergoing partial decomposition (600-Li25, 600-Na25 and 600-K25 samples), a strong linear correlation shows up (Fig. 10). Nevertheless, the 600-Cs25 sample, the only catalyst from the same series that barely decomposes, veers slightly away from the linearity. Similar linearity deviation applies to the K-doped catalyst activated at 500 °C (500-K25), with no apparent decomposition, like the 600-Cs25 sample.

It has been previously reported that surface of MoVSb mixed oxide catalysts present both Brönsted and Lewis acid sites [32,36,38], so that, according with catalytic and characterization results obtained, the strongest acid sites removed by alkali metal incorporation are mainly Brönsted sites, while some weaker Lewis acid sites remain (Fig. 2 and Table 1). Anyway, although the decrease in the number and strength of acid sites appears paramount for the high ethylene selectivity achieved on the MoVSb mixed oxide catalysts doped with alkali metals, it does not completely justify all the differences in selectivity observed among the different doped catalysts. Therefore, other aspects should be considered. In this way, it has been already reported [40] that no phase decomposition appears when activation after alkali metal impregnation is made at 500 °C/ $\text{N}_2$ , whereas activation at 600 °C/ $\text{N}_2$  leads to a partial decomposition of original crystalline structures (M1 and M2 phases) in a different proportion depending on the alkali metal added. Thus,

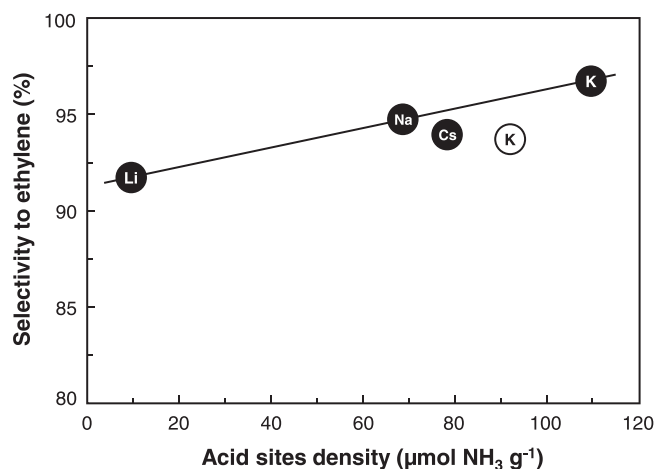


Fig. 10. Selectivity to ethylene (at ethane isoconversion of c.a. 30 %) versus concentration of acid sites per mass unit of alkali doped MoVSb mixed oxide catalysts activated at 600 °C (●) and the K-doped one activated at 500 °C (○). Accurate values for acid sites density in Table 1.

decomposition decreases as increasing the cation size of the impregnated alkali metal (Fig. 1) up to cesium for which practically no decomposition is observed. That means, alkali metals added are not only modifying the catalyst surface but also influencing on the structural catalyst stability probably due to their partial incorporation into framework hollows.

The optimal behavior in both reactions (ethane ODH and propane selective oxidation) has been observed to be reached for the K-doped MoVSb catalyst activated at 600 °C (600-K25 sample) where M2 phase decomposes with the minimum decomposition of M1 active phase. At this point, it must be indicated that M2 phase with Mo-V-Sb composition was determined to have a negative effect on the selectivity to acrylic acid in propane partial oxidation [34,40,50]. By contrast, the presence of M2 phase has been proved not to influence on the selectivity to ethylene for ethane ODH [12,52]. Nevertheless, the absence of M1 phase is important in terms of alkane conversion [34–37,40,50], since it is considered as the unique phase responsible for the alkane activation in this type of catalytic systems. While M2 phase has shown not to be active for ethane or propane activation [35,57]. In this sense, the results for ethane conversion depending on the type of alkali metal doping the MoVSbO catalyst (Fig. 5) are in good agreement with those obtained for the partial decomposition of M1 phase (Fig. 1). Thus, the higher the degree of M1 decomposition, the lower the ethane conversion.

## 5. Conclusions

The modification of a conventional Mo-V-Sb mixed oxide catalyst, through a post-synthesis treatment based on the incorporation of very low amount of alkali metal cations (Li, Na, K or Cs) by wet impregnation, produces in all cases important changes in the catalytic properties of the resulting materials for ODH of ethane, improving considerably the selectivity to ethylene at high ethane conversion, with some differences depending on the alkali metal incorporated. The amount of alkali metal, but also the activation temperature after the alkali metal incorporation also influences on the physicochemical and catalytic properties of the final material. Thus, the best results are reached doping with  $\text{K}^+$  using a molar K/Mo ratio of 0.0025, and an activation temperature of 600 °C. The resulting K-doped catalyst presents yields to ethylene around 70 %, much higher than those reported for any other Mo-V-Sb-O catalyst [26, 28,51,52] and comparable to the yield achieved with the most effective Mo-V-Te-Nb-O catalysts previously described [12,13,26,52–55]. This fact has an additional value since the possibility of obtaining an effective catalytic material for ethane ODH without containing niobium implies an important reduction in the cost price of catalyst preparation.

According with the results achieved, it can be concluded that factors improving catalytic behavior of alkali metal doped MoVSbO-based catalysts for partial oxidation of propane to acrylic acid, also influence in a similar way on their catalytic properties for ODH of ethane to ethylene. In this way, the results show that, although M1 phase presence is necessary to obtain high selectivity to ethylene, M2 phase decomposition and surface modification of M1 phase, especially the decrease in the number and strength of surface acid sites, are key factors to remove and/or block active sites leading to CO and  $\text{CO}_2$  formation. From a practical point of view, yields to ethylene obtained with the optimum K-doped catalyst (c.a. 70 %) on ethane ODH are higher than those from steam cracking process; although productivity should be improved in order to get an alkane-based process competitive enough [56].

## CRedit authorship contribution statement

F. Ivars-Barceló: Conceptualization, Investigation, Formal analysis, Visualization, Funding acquisition, Writing - original draft. B. Solsona: Investigation, Formal analysis. E. Asedegbega-Nieto: Investigation, Formal analysis. J.M. López Nieto: Conceptualization, Funding acquisition, Project administration, Resources, Supervision, Validation.

## Declaration of Competing Interest

The authors declare that they have no known competing financial interests or personal relationships that could have appeared to influence the work reported in this paper.

## Data availability

The data that has been used is confidential.

## Acknowledgments

This work was supported by the Ministerio de Ciencia e Innovación of Spain (projects PID21-126235OB-C31 and PID21-126235OB-C33). F. Ivars-Barceló also acknowledges the Ministerio de Ciencia e Innovación of Spain by the support from the “Ramón y Cajal” excellence grant (Ref.: RYC2020-029470-I/AEI/10.13039/501100011033).

## Appendix A. Supporting information

Supplementary data associated with this article can be found in the online version at [doi:10.1016/j.apcata.2023.119200](https://doi.org/10.1016/j.apcata.2023.119200).

## References

- R.C. Schucker, G. Dimitrakopoulos, K. Derrickson, K.K. Kopeć, F. Alahmadi, J. R. Johnson, L. Shao, A.F. Ghoniem, Oxidative dehydrogenation of ethane to ethylene in an oxygen-ion-transport-membrane reactor: a proposed design for process intensification, *Ind. Eng. Chem. Res.* 58 (2019) 7989–7997.
- B. Subramaniam, R.K. Helling, C.J. Bode, Quantitative sustainability analysis: a powerful tool to develop resource-efficient catalytic technologies, *ACS Sust. Chem. Eng.* 4 (2016) 5859–5865.
- S.M. Sadrameli, Thermal/catalytic cracking of hydrocarbons for the production of olefins: a state-of-the-art review I: Thermal cracking review, *Fuel* 140 (2015) 102–115.
- C.R. Riley, A. De La Riva, I.L. Ibarra, A.K. Datye, S.S. Chou, Achieving high ethylene yield in non-oxidative ethane dehydrogenation, *Appl. Catal. A-Gen.* 624 (2021), 118309.
- T. Ren, M. Patel, K. Blok, Olefins from conventional and heavy feedstocks: energy use in steam cracking and alternative processes, *Energy* 31 (2006) 425–451.
- Y. Gao, L. Neal, D. Ding, W. Wu, C. Baroi, A.M. Gaffney, F. Li, Recent advances in intensified ethylene production—a review, *ACS Catal.* 9 (2019) 8592–8621.
- A.M. Gaffney, J.W. Sims, V.J. Martin, N.V. Duprez, K.J. Louthan, K.L. Roberts, Evaluation and analysis of ethylene production using oxidative dehydrogenation, *Catal. Today* 369 (2021) 203–209.
- S. Najari, S. Saeidi, P. Concepcion, D.D. Dionysiou, S.K. Bhargava, A.F. Lee, K. Wilson, Oxidative dehydrogenation of ethane: catalytic and mechanistic aspects and future trends, *Chem. Soc. Rev.* 50 (2021) 4564–4605.
- J.T. Grant, J.M. Venegas, W.P. McDermott, I. Hermans, Aerobic oxidations of light alkanes over solid metal oxide catalysts, *Chem. Rev.* 118 (2018) 2769–2815.
- F. Cavani, A. Chiericato, J.M. López Nieto, J.-M.M. Millet, in: A.J.L. Pombeiro, M. F.C. Guedes da Silva (Eds.), *Alkane Functionalization*, John Wiley & Sons Ltd, 2019, pp. 159–188.
- C.A. Gärtner, A.C. vanVeen, J.A. Lercher, Oxidative dehydrogenation of ethane: common principles and mechanistic aspects, *ChemCatChem* 5 (2013) 3196–3217.
- P. Botella, E. Garcia-Gonzalez, A. Dejoz, J.M. López Nieto, M.I. Vázquez, J. Gonzalez-Calbet, Selective oxidative dehydrogenation of ethane on MoVTeNbO mixed metal oxide catalysts, *J. Catal.* 225 (2004) 428–438.
- A. de Arriba, G. Sánchez, R. Sánchez-Tovar, P. Concepción, R. Fernández-Domene, B. Solsona, J.M. López Nieto, On the selectivity to ethylene during ethane ODH over M1-based catalysts. A surface and electrochemical study, *Catal. Today* 418 (2023), 114122.
- Z.S. Han, X.D. Yi, Q. Xie, R.C. Li, H. Lin, Y.M. He, L.Q. Chen, W.Z. Weng, H.L. Wan, Oxidative dehydrogenation of ethane over MoVTeNbO catalyst prepared by a slurry method, *Chin. J. Catal.* 26 (2005) 441–442.
- T.T. Nguyen, B. Deniau, P. Delichere, J.-M.M. Millet, Influence of the content and distribution of vanadium in the M1 phase of the MoVTe(Sb)NbO catalysts on their catalytic properties in light alkanes oxidation, *Top. Catal.* 57 (2014) 1152–1162.
- T. Konya, T. Katou, T. Murayama, S. Ishikawa, M. Sadakane, D. Buttrey, W. Ueda, An orthorhombic Mo<sub>3</sub>VO<sub>x</sub> catalyst most active for oxidative dehydrogenation of ethane among related complex metal oxides, *Catal. Sci. Technol.* 3 (2013) 380–387.
- J.S. Valente, R. Quintana-Solórzano, H. Armendáriz-Herrera, G. Barragán-Rodríguez, J.M. López-Nieto, Kinetic study of oxidative dehydrogenation of ethane over MoVTeNb mixed-oxide catalyst, *Ind. Eng. Chem. Res.* 53 (2014) 1775–1786.
- P. Kube, B. Frank, S. Wrabetz, J. Kröhnert, M. Hävecker, J. Velasco-Vélez, J. Noack, R. Schlögl, A. Trunschke, Functional analysis of catalysts for lower alkane oxidation, *ChemCatChem* 9 (2017) 573–585.
- L. Annamalai, Y. Liu, S. Ezenwa, Y. Dang, S.L. Suib, P. Deshlahra, Influence of tight confinement on selective oxidative dehydrogenation of ethane on MoVTeNb mixed oxides, *ACS Catal.* 8 (2018) 7051–7067.
- D. Melzer, G. Mestl, K. Wanninger, Y. Zhu, N.D. Browning, M. Sanchez-Sanchez, J. A. Lercher, Design and synthesis of highly active MoVTeNb-oxides for ethane oxidative dehydrogenation, *Nat. Commun.* 10 (2019) 4012.
- H. Tsuji, Y. Koyasu, Synthesis of MoVNBTe(Sb)O<sub>x</sub> composite oxide catalysts via reduction of polyoxometalates in an aqueous medium, *J. Am. Chem. Soc.* 124 (2002) 5608–5609.
- J.M.M. Millet, H. Roussel, A. Pigamo, J.L. Dubois, J.C. Jumas, Characterization of tellurium in MoVTeNbO catalysts for propane oxidation or ammoxidation, *Appl. Catal. A-Gen.* 232 (2002) 77–92.
- P. Botella, J.M. López Nieto, B. Solsona, A. Mifsud, F. Marquez, The preparation, characterization, and catalytic behavior of MoVTeNbO catalysts prepared by hydrothermal synthesis, *J. Catal.* 209 (2002) 445–455.
- D. Vitry, Y. Morikawa, J.L. Dubois, W. Ueda, Mo-V-Te-(Nb)-O mixed metal oxides prepared by hydrothermal synthesis for catalytic selective oxidations of propane and propene to acrylic acid, *Appl. Catal. A-Gen.* 251 (2003) 411–424.
- P. DeSanto, D.J. Buttrey, R.K. Grasselli, C.G. Lugmair, A.F. Volpe, B.H. Toby, T. Vogt, Structural characterization of the orthorhombic phase M1 in MoVNBTeO propane ammoxidation catalyst, *Top. Catal.* 23 (2003) 23–38.
- W. Ueda, K. Oshihara, Selective oxidation of light alkanes over hydrothermally synthesized Mo-V-M-O (M=Al, Ga, Bi, Sb, and Te) oxide catalysts, *Appl. Catal. A-Gen.* 200 (2000) 135–143.
- W. Ueda, K. Oshihara, D. Vitry, T. Hisano, Y. Kayashima, Hydrothermal synthesis of Mo-based oxide catalysts and selective oxidation of alkanes, *Catal. Surv. Jpn.* 6 (2002) 33–44.
- P. Botella, A. Dejoz, J.M. López Nieto, P. Concepción, M.I. Vázquez, Selective oxidative dehydrogenation of ethane over MoVSbO mixed oxide catalysts, *Appl. Catal. A-Gen.* 298 (2006) 16–23.
- C. Xin, F. Wang, G.Q. Xu, Tuning surface V<sup>5+</sup> concentration in M1 phase MoVSbOx catalysts for ethylene production from ethane through oxidative dehydrogenation reaction, *Appl. Catal. A-Gen.* 610 (2021), 117946.
- J. Sánchez Valente, J.M. López Nieto, H. Armendariz Herrera, A. Massó Ramírez, F. Ivars Barceló, Md.L.A. Guzman Castillo, R. Quintana Solórzano, A. Rodríguez Hernández, V. Paz del Angel, M. Flores Eitel, Oxidative dehydrogenation of ethane to ethylene and preparation of multimetallic mixed oxide catalyst for such process, *US Pat. 9409156 B2* (2016); assigned to PEMEX-IMP-UPV.
- J.M.M. Millet, M. Baca, A. Pigamo, D. Vitry, W. Ueda, J.L. Dubois, Study of the valence state and coordination of antimony in MoVSbO catalysts determined by XANES and EXAFS, *Appl. Catal. A-Gen.* 244 (2003) 359–370.
- M. Baca, A. Pigamo, J.L. Dubois, J.M.M. Millet, Fourier transform infrared spectroscopic study of surface acidity by pyridine adsorption on the M1 active phase of the MoVTe(Sb)NbO catalysts used in propane oxidation, *Catal. Commun.* 6 (2005) 215–220.
- V.V. Gulians, R. Bhandari, B. Swaminathan, V.K. Vasudevan, H.H. Brongersma, A. Knoester, A.M. Gaffney, S. Han, Roles of surface Te, Nb, and Sb oxides in propane oxidation to acrylic acid over orthorhombic Mo-V-O phase, *J. Phys. Chem. B* 109 (2005) 24046–24055.
- F. Ivars, B. Solsona, E. Rodríguez-Castellón, J.M. López Nieto, Selective propane oxidation over MoVSbO catalysts. On the preparation, characterization and catalytic behavior of M1 phase, *J. Catal.* 262 (2009) 35–43.
- B. Deniau, G. Bergeret, B. Jouguet, J.L. Dubois, J.M.M. Millet, Preparation of single M1 phase MoVTe(Sb)NbO catalyst: study of the effect of M2 phase dissolution on the structure and catalytic properties, *Top. Catal.* 50 (2008) 33–42.
- P. Concepción, P. Botella, J.M. López Nieto, Catalytic and FT-IR study on the reaction pathway for oxidation of propane and propylene on V- or Mo-V-based catalysts, *Appl. Catal. A-Gen.* 278 (2004) 45–56.
- J.M. López Nieto, B. Solsona, P. Concepcion, F. Ivars, A. Dejoz, M.I. Vazquez, Reaction products and pathways in the selective oxidation of C<sub>2</sub>-C<sub>4</sub> alkanes on MoVTeNb mixed oxide catalysts, *Catal. Today* 157 (2010) 291–296.
- T. Blasco, P. Botella, P. Concepción, J.M. López Nieto, A. Martínez-Arias, C. Prieto, Selective oxidation of propane to acrylic acid on K-doped MoVSbO catalysts: catalyst characterization and catalytic performance, *J. Catal.* 228 (2004) 362–373.
- W. Ueda, Y. Endo, N. Watanabe, K-doped Mo-V-Sb-O crystalline catalysts for propane selective oxidation to acrylic acid, *Top. Catal.* 38 (2006) 261–268.
- F. Ivars, B. Solsona, P. Botella, M.D. Soriano, J.M. López Nieto, Selective oxidation of propane over alkali-doped Mo-V-Sb-O catalysts, *Catal. Today* 141 (2009) 294–299.
- O.V. Safonova, B. Deniau, J.M.M. Millet, Mechanism of the oxidation-reduction of the MoVSbNbO catalyst: In operando X-ray absorption spectroscopy and electrical conductivity measurements, *J. Phys. Chem. B* 110 (2006) 23962–23967.
- T.M.N. Le, R. Checa, P. Bargiela, M. Aouine, J.M.M. Millet, New synthesis of pure orthorhombic Mo-V-A oxide phases, where A = Sb, Bi and Pb, and testing for the oxidation of light alkanes, *J. Alloy. Comp.* 910 (2022), 164745.
- V. Rakić, L. Damjanović, in: A. Auroux (Ed.), *Calorimetry and Thermal Methods in Catalysis*, Springer Berlin Heidelberg, Berlin, Heidelberg, 2013, pp. 131–174.
- I. Chorkendorff, J.W. Niemantsverdriet, *Concepts of Modern Catalysis and Kinetics*, ch.7, Wiley, 2003, pp. 267–299.
- R. Grabowski, B. Grzybowska, A. Kozłowska, J. Słoczyński, K. Wcisło, Y. Barbaux, Effect of alkali metals additives to V<sub>2</sub>O<sub>5</sub>/TiO<sub>2</sub> catalyst on physicochemical properties and catalytic performance in oxidative dehydrogenation of propane, *Top. Catal.* 3 (1996) 277–288.
- R.B. Watson, U.S. Ozkan, Propane and propylene adsorption effects over MoOx-based catalysts induced by low levels of alkali doping, *J. Mol. Catal. A-Chem.* 194 (2003) 115–135.



- [47] P. Botella, P. Concepcion, J.M. López Nieto, B. Solsona, Effect of potassium doping on the catalytic behavior of Mo-V-Sb mixed oxide catalysts in the oxidation of propane to acrylic acid, *Catal. Lett.* 89 (2003) 249–253.
- [48] R.B. Watson, U.S. Ozkan, Spectroscopic and structural characterization of low-level alkali doping effects on Mo/silica-titanic catalysts, *J. Phys. Chem. B* 106 (2002) 6930–6941.
- [49] G. Centi, G. Golinelli, G. Busca, Modification of the surface pathways in alkane oxidation by selective doping of bronsted acid sites of vanadyl pyrophosphate, *J. Phys. Chem.* 94 (1990) 6813–6819.
- [50] F. Ivars, B. Solsona, M.D. Soriano, J.M. Lopez Nieto, Selective oxidation of propane over AMoVSbO catalysts (A = Li, Na, K, Rb or Cs), *Top. Catal.* 50 (2008) 74–81.
- [51] Q. Xie, L.Q. Chen, W.Z. Weng, H.L. Wan, Preparation of MoVTe(Sb)Nb mixed oxide catalysts using a slurry method for selective oxidative dehydrogenation of ethane, *J. Mol. Catal. A-Chem.* 240 (2005) 191–196.
- [52] P. Botella, A. Dejoz, M.C. Abello, M.I. Vazquez, L. Arrua, J.M.L. Nieto, Selective oxidation of ethane: Developing an orthorhombic phase in Mo-V-X (X = Nb, Sb, Te) mixed oxides, *Catal. Today* 142 (2009) 272–277.
- [53] J.M. López Nieto, P. Botella, M.I. Vazquez, A. Dejoz, The selective oxidative dehydrogenation of ethane over hydrothermally synthesised MoVTeNb catalysts, *Chem. Commun.* (2002) 1906–1907.
- [54] F. Ivars, P. Botella, A. Dejoz, J.M. López Nieto, P. Concepción, M.I. Vázquez, Selective oxidation of short-chain alkanes over hydrothermally prepared MoVTeNbO catalysts, *Top. Catal.* 38 (2006) 59–67.
- [55] J.M. López Nieto, P. Botella, P. Concepcion, A. Dejoz, M.I. Vázquez, Oxidative dehydrogenation of ethane on Te-containing MoVNbO catalysts, *Catal. Today* 91–92 (2004) 241–245.
- [56] S.T. Oyama, Adsorbate bonding and the selection of partial and total oxidation pathways, *J. Catal.* 128 (1991) 210–217.
- [57] P. Botella, J.M. López Nieto, B. Solsona, Preparation, characterisation, and catalytic behaviour of a new TeVMoO crystalline phase, *Catal. Lett.* 78 (2002) 383–387.